Cross-bridge attachment and stiffness during isotonic shortening of intact single muscle fibers

P. J. Griffiths,* C. C. Ashley,* M. A. Bagni,‡ Y. Maéda,§ and G. Cecchi‡

*University Laboratory of Physiology, Oxford, OX1 3PT UK;
‡Dipartimento di Scienze Fisiologiche, Università degli Studi di Firenze, Florence, I-50134 Italy;
§EMBL Outstation, Deutsches Elektronen-Synchrotron, D-2000 Hamburg 52, Germany

ABSTRACT Equatorial x-ray diffraction pattern intensities (I_{10} and I_{11}), fiber stiffness and sarcomere length were measured in single, intact muscle fibers under isometric conditions and during constant velocity (ramp) shortening. At the velocity of unloaded shortening (V_{max}) the I_{10} change accompanying activation was reduced to 50.8% of its isometric value, I_{11} reduced to 60.7%. If the roughly linear relation between numbers of attached bridges and equatorial signals in the isometric state also applies during shortening, this would predict 51–61% attachment. Stiffness (measured using 4 kHz sinusoidal length oscillations), another putative measure of bridge attachment, was 30% of its isometric value at V_{max}. When small step length changes were applied to the preparation (such as used for construction of T1 curves), no equatorial intensity changes could be detected with our present time resolution (5 ms).

Therefore, unlike the isometric situation, stiffness and equatorial signals obtained during ramp shortening are not in agreement. This may be a result of a changed crossbridge spatial orientation during shortening, a different average stiffness per attached crossbridge, or a higher proportion of single headed crossbridges during shortening.

INTRODUCTION

In striated muscle the proteins actin and myosin are arranged as interdigitating filaments axially along the muscle cells. According to the widely accepted cross-bridge theory of muscle contraction (1–3), force follows the attachment of crossbridges (periodic projections from the surface of the myosin filaments) to the actin filaments. Attachment is accompanied by an increase in fiber instantaneous stiffness and a change in the equatorial x-ray diffraction pattern from the quasi-crystalline arrangement of the protein filaments (4). In the isometric state, the equatorial intensity changes accompanying activation are proportional to axial force (5), and are therefore thought to indicate the proportion of cycling bridges. Instantaneous stiffness changes upon activation are thought to arise from an elastic component associated with each individual attached crossbridge, hence stiffness may also indicate the degree of crossbridge attachment. We have recently reported the first successful application of time-resolved x-ray diffraction to intact single muscle fibers under isometric conditions (6). We found good agreement between the time course of changes in equatorial signals and fiber stiffness both during activation and isometric relaxation. We have now extended our observations to the isotonic condition.

Previous studies on whole muscle under isotonic conditions (i.e., during shortening at constant force) suggested that equatorial intensities are either unchanged or increase slightly (7) or change towards their resting levels by more than 50% of their plateau values during shortening at V_{max} (8). However, stiffness measurements suggest a larger change in the proportion of attached bridges during muscle shortening (a decline of 70% as indicated in references 9–11), suggesting that the proportion of attached crossbridges indicated by stiffness and equatorial intensities may not be in agreement under isotonic conditions. Recent motility assays of isolated contractile systems suggest that the fraction of attached bridges may even increase during shortening (12, 13). Clearly, any model of the crossbridge cycle must predict the proportion of attached bridges during shortening, and so the determination of this proportion is of great importance. But comparison of previous studies of the fraction of attached bridges during shortening in living fibers is complicated by the difference in the preparations (whole muscle versus single fibers) and species used for x-ray diffraction and stiffness measurements. In addition, precise control and measurement of shortening velocity in whole muscle experiments is difficult, and must involve a margin of error. There are also no data showing complementary stiffness and x-ray measurements during the same experiment. We have therefore studied the behavior of stiffness and equatorial intensities during shortening in single intact muscle fibers of the frog, where time resolved sarcomere length, x-ray diffraction, and mechanical measurements can be made on the same preparation, and the complications of a multicellular preparation are avoided. We find that indeed stiffness and equatorial signals do not agree, stiffness consistently reporting a smaller fraction of bridges in an attached state.

Address correspondence to Dr. P. J. Griffiths, University Laboratory of Physiology, University of Oxford, Parks Road, Oxford, England OX1 3PT, United Kingdom.

METHODS

a) Experimental protocol

Single muscle fibers isolated from the tibialis anterior muscle of frogs (*Rana temporaria*) were mounted in a chamber and positioned in the

0006-3495/93/04/1150/11 $2.00

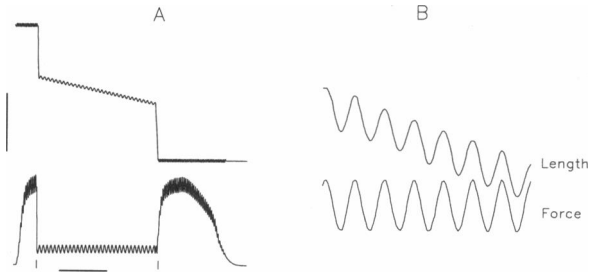

FIGURE 1 Measurement of tension and stiffness during fiber shortening. (*A*) ramp shortening (*upper trace*) with superimposed sinusoidal length oscillations at 3 kHz. applied at the plateau of a tetanic tension (*lower panel*); (*B*) expansion of a central portion of the records in (*A*) to show length (*upper trace*) and force (*lower trace*) oscillations. Note the absence of phase shift between records. Over the period during which the fiber was shortening, the sampling rate of the oscilloscope was increased to 0.1 μs^{-1}, elsewhere the sampling rate was 1 ms^{-1}. This change of sampling rate enabled us to record the whole force response while having adequate time resolution during the period of shortening. Vertical calibration: (*A*) 178 $kN \cdot m^{-2}$ or 3.2% l_0, (*B*) 27 $kN \cdot m^{-2}$ or 0.23% l_0. Horizontal calibration: (*A*) 2 ms between the two small vertical bars, 20 ms outside, (*B*) 570 μs.

x-ray beam from the source DORIS (beam dimensions 4 × 0.3 mm, $\lambda = 0.15$ nm). Chamber temperature was maintained at 4°C. Aluminium clips on the tendons to reduce series compliance were used to mount the fiber horizontally between a moving coil motor and a capacitance transducer. The position of the fiber in the x-ray windows was adjusted until central and horizontal, then the whole chamber was raised or lowered in small steps until the height corresponding to the strongest diffraction pattern was found. Throughout this alignment procedure, the x-ray beam was greatly attenuated to avoid fiber damage. The design of the chamber and the details of the beamline have been published elsewhere (6). The fiber was then electrically stimulated (stimulation frequency 20 Hz) to induce a tetanus of 400 ms duration. At the plateau of the tetanus a period of constant velocity (i.e., ramp) shortening was initiated. This was achieved using the motor under servo control to impose changes of length on the fiber at a predetermined velocity. The period of constant velocity shortening was preceded by a quick step release sufficient to discharge tension to the appropriate level for the chosen velocity of ramp shortening. Total shortening was not greater than 9% of initial fiber length (l_0), and the initial sarcomere length was chosen so that throughout the period of shortening fibers remained within the plateau region of the length–tension relationship. Shortening velocity was controlled by a moving coil motor capable of completing a step within 100 μs. Our isotonic shortening protocol was repeated at 3 minute intervals, collecting equatorial intensity levels every 5 ms for subsequent averaging. Typically, 10 to 20 tetani were required to collect sufficient counts for analysis of the equatorial intensity changes. In some fibers, after about half the required number of tetani had been recorded, a series of tetani with length oscillations was obtained to determine fiber stiffness during shortening. Stiffness was calculated from the force response to 4 kHz sinusoidal length oscillations of 0.05% l_0 peak to peak in amplitude. Force was recorded using a capacitance force transducer (50 kHz resonant frequency). Care was taken to ensure that no phase shift could be detected between force and length signals during stiffness measurements, which would indicate fiber resonance (14). If a phase shift was detected, the frequency of the length oscillations was slightly reduced. An example of the protocol for stiffness measurement in shown in Fig. 1. Throughout the experiment, sarcomere length in the center of the region of the fiber exposed to the x-ray beam was monitored using a laser diffractometer system (6), and time resolved sarcomere length changes were recorded simultaneously with the force and intensity data.

Equatorial patterns were collected on a one-dimensional crossed wire detector (15). Counts from 128 output channels were stored (together with sarcomere length, fiber length, beam intensity and force) in a local VAX 11/750 computer.

b) Data analysis

The intensity of reflections is proportional to the square of the quantity of mass in the beam. Because shortening of the fiber introduces more mass into the beam, necessarily introducing a movement artifact into the intensity of the reflections, some correction strategy was required to remove this effect. For example, fiber shortening by 5% of its length would introduce 5% more mass into the beam, with consequent 10.25% elevation of intensities. Previous studies of equatorial intensity dependence on sarcomere length (4) have avoided this difficulty by plotting the ratio of I_{10} to I_{11}, but this results in loss of information about the behavior of individual reflections which we wished to retain.

A correction strategy could be to estimate the extent of individual artifacts separately. For example, as changes in sarcomere length during shortening are known from our sarcomere length records, a correction for increasing mass in the beam during shortening could be applied. Since beam intensity is also continuously monitored during the experiment, a further correction for fluctuations in beam intensity is also possible. However, multiple corrections of this nature may introduce more errors than they remove, since the effects of incorrect estimation of each artifact become cumulative. This approach also assumes knowledge of the source of all artifacts and the availability of a suitable correction procedure for each (which is not available, for example, in the case of vertical displacement of the fiber). Instead we chose a different strategy. For each time frame in an experiment we calculated the "spectrum intensity," the integrated intensity over the whole portion of the equatorial pattern recorded by the detector. Each frame was then normalized for its spectrum intensity to give a constant spectrum intensity throughout the experiment. In this strategy we assumed that the spectrum intensity, after correction for all shortening artifacts, would have remained constant. This assumption is not based on any theoretical grounds, but on experimental observations. Our previous experience with isometric contractions (6) indicated that spectrum intensity changed little upon activation of fibers in which little movement occurred (as indicated by the sarcomere pattern). This procedure should correct for fluctuations in beam intensity, fiber shortening, and vertical displacement, and permit comparisons of spectra to be made when experimental parameters are being varied in successive experiments on the same fiber (e.g., changes of sarcomere length or shortening velocity).

The time course of intensity changes were measured either by integration of whole areas (including background) below the peaks (6), or by a curve fitting procedure (16) which excluded the contribution of background intensity. Ignoring differences in noise levels and absolute intensities, the two methods gave essentially identical time courses and relative magnitudes of intensity changes. The curve fitting method first obtains estimates of intensity levels from an exponential background subtraction (fitted by eye) from the original spectrum, then uses these estimates as starting points to fit 6 Gaussians (10, 11, 20, 21, 30, and *Z*) to each half of the original pattern, with suitable expressions for the background. The form of the model used for fitting was therefore:

$$y(x) = a_1 + a_2 x + a_3 x^2 + a_4 \exp(a_5 x) + \sum_{i=1}^{n=6} \frac{b_i \exp((x-\mu_i)/4\sigma_i)^2}{\sigma_i (2\pi)^{1/2}}$$

where x is the distance from the origin of the pattern to the centre of reflection i, $y(x)$ the intensity of the spectrum at x, a_is the constants defining the background, and b_i, μ_i and σ_i the area, mean, and stan-

dard deviation of each of the 6 Gaussians. The positions of 10, 20, and 30 are fitted as integer multiples of the 10 spacing, while 11, 21, and Z spacings are treated as independent variables. All figures showing changes in intensity have decreases in 10 intensity plotted upwards to aid comparison with the 11 and tension signals.

Unless otherwise stated, mean values of quantities are quoted plus or minus the standard deviation.

Stiffness was calculated as the ratio of the peak to peak amplitudes of force and length changes during the 4 kHz sinusoidal oscillations. Force and length signals were recorded on a Nicolet 2082 digital oscilloscope because of the much higher time resolution required in the analysis of stiffness data (Fig. 1).

RESULTS

Upon stimulation of the fiber to produce an isometric tetanus, the 10 equatorial intensity (I_{10}) fell by 46.5 ± 2.5% and 11 intensity (I_{11}) increased by 139.7 ± 26.9% at a sarcomere length of 2.2 μm (I_{10} and I_{11} calculated as the area of the respective reflections). Only the fitted spectrum procedure was used to obtain these values, since background intensity is not included in reflection intensities when using this method. These means include only data from fibers used for the present analysis of the effects of shortening, but are consistent with the I_{10}/I_{11} intensity ratios reported in our previous work on fibers in the isometric state (6). We shall refer to these intensity changes as the "equatorial signals."

We then tested the validity of our assumption that corrected total spectrum intensity would not change during a contraction, the basis of our corrections for movement artifacts. Under isometric conditions, the spectrum intensity remains virtually constant during the transition from activation to relaxation, as we had observed previously (6). As will be shown, the recovery from isotonic shortening to a new tetanus plateau also occurs under isometric conditions, and we found that this recovery also occurs without appreciable change in total spectrum intensity. However, since shortening introduces extra mass into the beam, one cannot expect uncorrected total spectrum intensity to remain constant when sarcomere length is being changed. We therefore examined the static spectra from relaxed fibers over a range of sarcomere lengths, and corrected the total spectrum intensity for incident beam intensity and total mass exposed to the beam (inversely proportional to the sarcomere length change). Since these measurements were static, fiber alignment in the beam could be optimized before each measurement, and hence the effects of vertical displacement of the fiber are removed (which is not possible during time resolved measurements). Our findings are shown in Fig. 2. Over the range of sarcomere lengths examined, a small increase in total spectrum intensity could be detected (0.32 per micron sarcomere length). Since our range of shortening did not exceed 9% l_0 only a 6% reduction of total spectrum intensity can be expected as a result of shortening in our time resolved isotonic data. Furthermore, since an increase in fiber

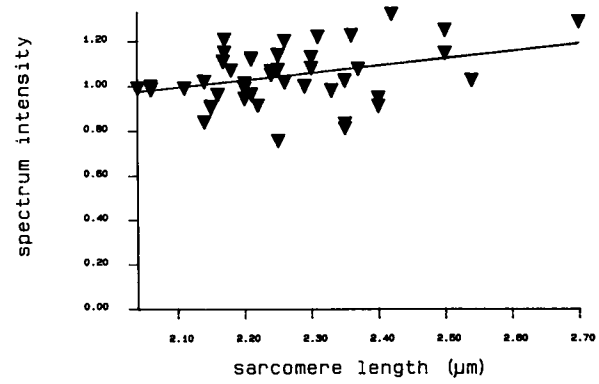

FIGURE 2 Total spectrum intensity (total detector counts) versus sarcomere length. Data obtained from 8 fibers. Total spectrum intensity expressed as a fraction of that at a sarcomere length of 2.06 μm sarcomere length. The spectrum intensity was corrected for main beam intensity and for the mass of fiber exposed to the beam, taking the beam intensity and mass exposed to be unity at the normalizing sarcomere length (2.06 μm). A linear regression fit of the data yielded the line shown on the figure, whose slope is 0.320 ± 0.237 μm^{-1} (95% confidence interval).

length is accompanied by a decrease in fiber radius, causing an increase in fiber mass in the most intense region of the beam, this 6% reduction of total spectrum intensity during shortening may be a slight overestimate of the effect, and so we believe our correction procedure based on the assumption of constant total spectrum intensity during shortening to be justified.

Since under isotonic conditions, equatorial signals were to be recorded under conditions of changing sarcomere length, we first studied the effect of sarcomere length on I_{10} and I_{11} in both the activated and relaxed state under isometric conditions (Fig. 3). For consistency with our time-resolved data during shortening, all spectra from any given fiber have been normalized for total spectrum intensity. In the relaxed state, I_{10} changed little over the range of sarcomere lengths we examined, but I_{11} fell abruptly beyond a sarcomere length of 2.2 μm. Below 2.2 μm, I_{11} intensity variation with sarcomere length is similar to that of I_{10}. In the activated state I_{10} increased linearly with sarcomere length and I_{11} fell, apparently less steeply than in the relaxed state, although the range of sarcomere lengths we examined was rather shorter, and the decline is therefore less well defined.

When a fiber was allowed to shorten at a constant velocity after having reached the isometric tension plateau, equatorial signals were either unaffected or fell towards their levels in the resting fiber, depending on the shortening velocity. When the tetanized fiber shortened at velocities of less than 0.4 V_{max}, the 10 and 11 equatorial signals showed no detectable change from their levels at the tetanus plateau. As the velocity of shortening was increased from 0.4 V_{max} to V_{max}, 10 and 11 signals changed towards their levels in the relaxed fiber. Fig. 4 shows the spectra obtained in the relaxed, plateau, and

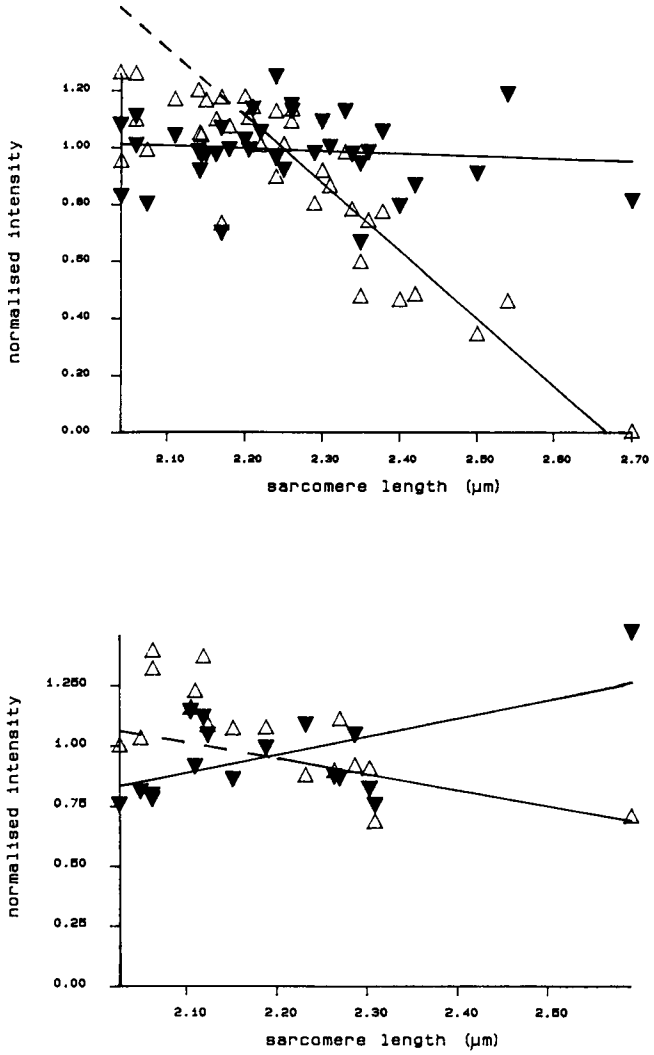

FIGURE 3 Equatorial intensities (I_{10}, ▼; I_{11}, △) versus sarcomere length in the relaxed (*upper panel*) and activated (*lower panel*) states under isometric conditions. All intensities determined by fitting Eq. 1 to the equatorial spectrum. Lines through the data points are linear regression fits over the whole range (I_{10}) or over the range above 2.2 μm (I_{11}) of sarcomere length values. Both 10 and 11 intensities have been normalized to their respective values at a sarcomere length of 2.2 μm for ease of data representation and to permit data from several fibers to be pooled. For this reason, the large absolute intensity differences between 10 and 11 reflections are not apparent in either the relaxed or the activated state. The fitted lines have slopes of $-0.09\ \mu m^{-1}$ (relaxed) and $0.76\ \mu m^{-1}$ (activated) for I_{10} points, and $-2.38\ \mu m^{-1}$ (relaxed) and $-0.66\ \mu m^{-1}$ (activated) for I_{11} points beyond 2.2 μm. The dashed part of the fitted line for I_{11} points is an extension of the fitted line obtained in the range of sarcomere lengths greater than 2.2 μm.

shortening states from the same fiber, with the best fit of the 6 Gaussian model superimposed. Shortening was permitted until the equatorial signals had reached a steady state level. The time required to attain a steady state level in equatorial intensities increased when the shortening velocity decreased, whereas force reached its steady state level almost immediately after the initial quick release (the amplitude of the release was chosen to reduce force to the appropriate isotonic level for the subsequent ramp). For example, when shortening at V_{max}, 90% of the steady state equatorial signals was reached within 25 ms (Fig. 5), while at 0.6 V_{max} 60 ms was required (Fig. 6). It can be seen that while the equatorial change in Fig. 5, obtained at close to V_{max} is quite pronounced, in Fig. 6 it is much less evident, despite a substantial reduction in tension. Because steady state intensities were reached after a delay during shortening, we compared the isometric and isotonic intensities obtained just before the end of the ramp and after the redevelopment of isometric tension. This method avoids any effects due to the change in sarcomere length which results from the shortening, since the recovery of tension after the ramp was found to occur under isometric conditions (as indicated by the output of our laser diffractometer system). However, it should be noted that changes in lattice spacing are associated with the redevelopment of tension under these conditions (17), and the influence of this on equatorial intensities during tension redevelopment is not fully understood. The distance shortened was such that the sarcomere length on termination of shortening was still within the range of full overlap, where intensity changes as a function of sarcomere length are small in the isometric state. On restoration of isometric conditions at the end of the ramp shortening, both 10 and 11 reflections recovered to their isometric levels with a shorter half-time of recovery than that observed for the redevelopment of isometric tension, as is also observed during the rise of tetanic tension. It has been shown that during redevelopment of tension following a period of shortening, the rise of stiffness also leads that of tension (18), and has a similar time course to that of the recovery of the equatorial signals shown here. The 11 reflection tended to reach or slightly overshoot its steady state isometric level somewhat faster than 10 during this recovery phase.

When stiffness was measured during identical conditions of shortening to those used for the intensity data, a much more pronounced effect of shortening velocity on stiffness was apparent. At 0.4 V_{max} stiffness was reduced to 55% of its plateau value, while at V_{max} the stiffness was reduced to 30% of plateau stiffness in agreement with earlier findings (9–11). In some fibers the effect of a quick step release (amplitude < 1% l_0, completed in 0.5 ms), rather than a ramp, was studied. Within the time resolution (5 ms) of our experiments no change in equatorial signals could be detected as a result of the step.

The variation of stiffness and equatorial signals with tension during shortening from 8 fibers is shown in Fig. 7. The upper panel shows the force–velocity relationship obtained for our data points and the associated fitted curve using a simple two state model (1). The lower panel shows intensity signals from 10 and 11 reflections and stiffness as a function of the force during shortening,

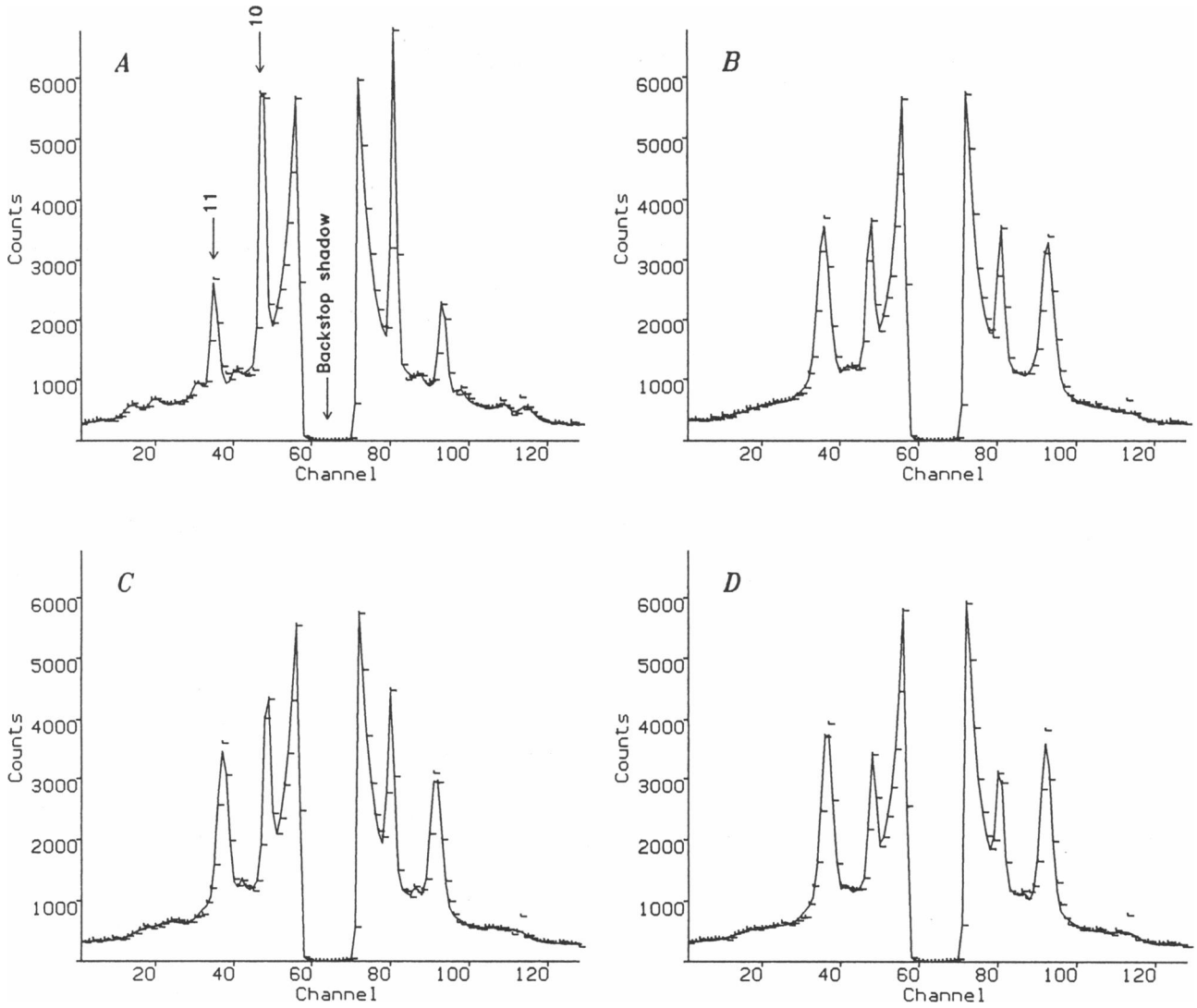

FIGURE 4 Equatorial patterns from the relaxed (*A*) and activated isometric fiber (*B*), during shortening (*C*), and after redevelopment of isometric tension on termination of shortening (*D*). The central region of each spectrum is the shadow of the backstop. Each spectrum was normalized for total spectrum intensity. Total exposure time 600 ms, average of 30 tetani. In the isotonic state, shortening velocity was 2.69 nm per half sarcomere per second. Individual points are counts in each channel, the continuous line is the fitted spectrum using the 6 Gaussian model.

normalized to a value of one in the activated isometric state, and zero in the resting state. The line in the lower panel close to the stiffness points is the predicted fraction of attached bridges based on the constants obtained from the upper panel. Because the quality of sarcomere length records was unsatisfactory in some fibers, velocity is plotted as fiber lengths per second so as to include all data available. It can be seen that the equatorial signals have similar values at a given force, while stiffness values are considerably smaller. The fitted intercept of the normalized I_{10} points on the ordinate axis has a value of 0.508, that of the normalised I_{11} points at 0.607 (this corresponds to shortening at V_{max}). If the relation between equatorial intensities and crossbridge attachment observed under isometric conditions can be applied during steady shortening, this result suggests that the number of attached crossbridges was reduced to 51–61% of the isometric situation when shortening at V_{max}. The stiffness points fall off below 0.1 P_0 because of the effects of tendon compliance, but points obtained above 0.1 P_0 can be extrapolated to their intercept on the ordinate at a value of about 0.3, in agreement with previous findings (9–11). This suggests that during shortening at V_{max} only 30% of crossbridges are attached, compared to the isometric condition.

DISCUSSION

The fraction of crossbridges attached during shortening is one of the parameters by which the values of rate constants used in models of muscle contraction are constrained. Whole muscle studies of equatorial intensity

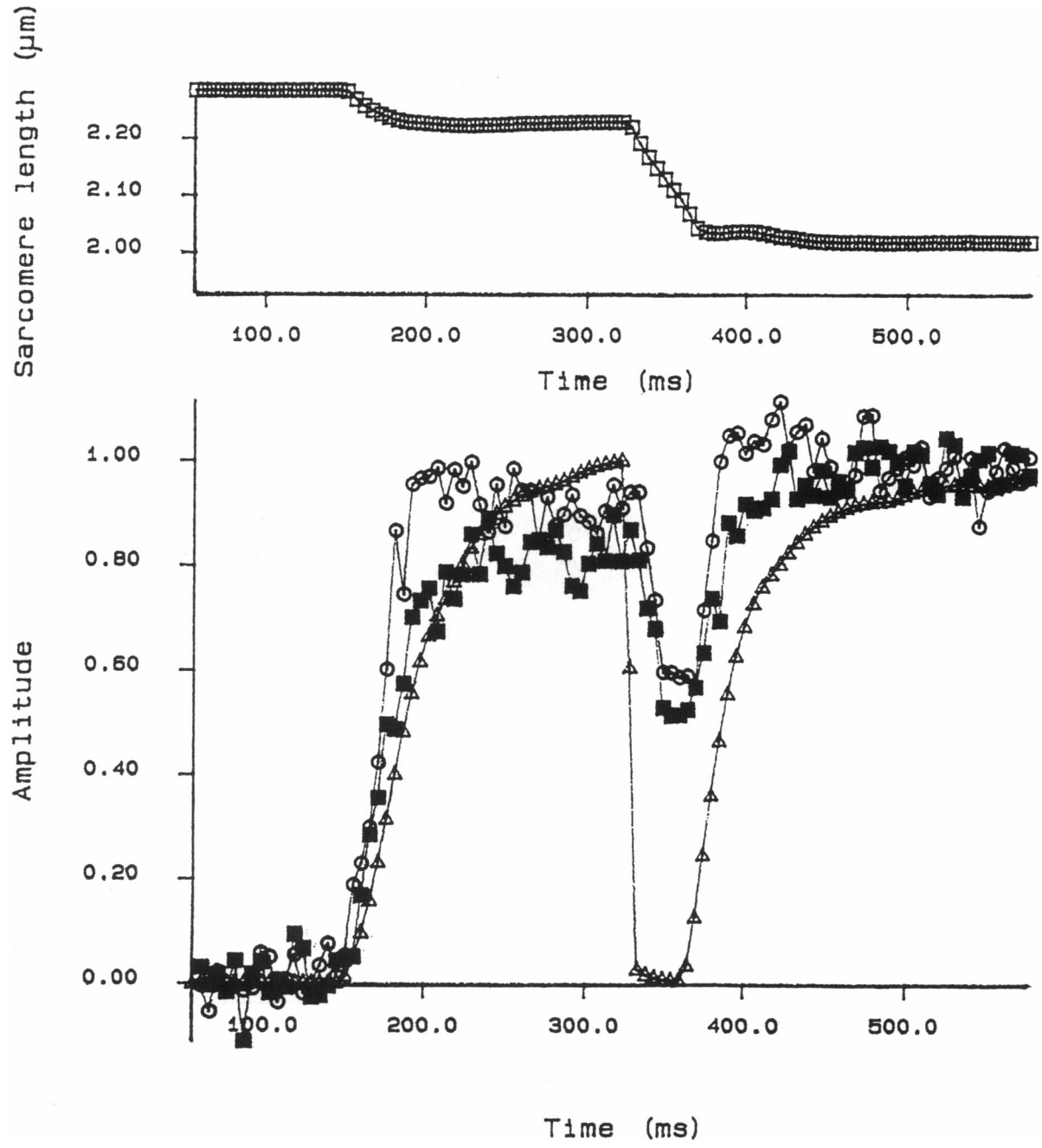

FIGURE 5 Sarcomere length (*top panel*), equatorial signals (I_{10}, ■; I_{11}, ○) and force (△) (*lower panel*) during isotonic shortening at close V_{max}. Electrical stimulation begins at the arrow. Shortening velocity 2.01 μm per half sarcomere per second. Intensities measured without background subtraction. Spectra normalized for integrated intensity. Camera length 4.8 m, average of 20 tetani. Sampling rate 5 ms. Sarcomere length monitored throughout tetanus by laser diffractometer system. Time in milliseconds.

changes during isotonic shortening have produced conflicting data, indicating either very little change (7) or a change of the order of 50% (8). Stiffness measurements during shortening have shown similar dependence of stiffness on shortening velocity to that reported here (9–11). That stiffness falls more gradually than tension can be accounted for by the presence of negatively strained bridges, which contribute to fiber stiffness but reduce tension. Hence at V_{max}, where tension is zero, cross-bridge attachment (and therefore stiffness) may be quite high. Motility assays suggest that during shortening, the fraction of attached bridges remains large, based on reduced force noise during shortening compared to the isometric state (12) and evidence of a relatively long working stroke time (13).

X-ray evidence from whole muscle experiments on

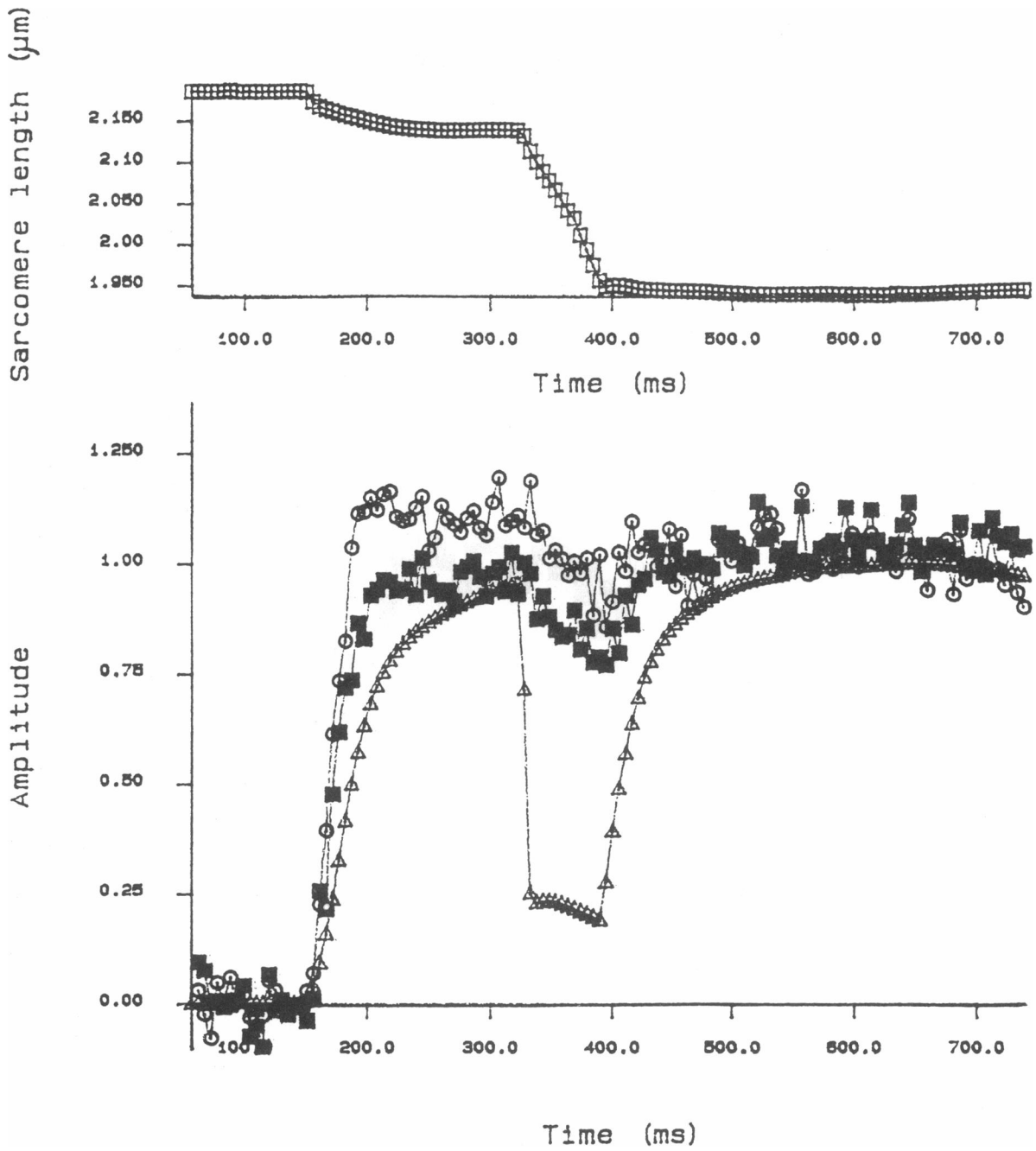

FIGURE 6 Sarcomere length, equatorial signals, and force during shortening at a velocity sufficient to reduce force to 0.2 P_0. Panels and symbols as in Fig. 1. Shortening velocity 1.39 μm per half sarcomere per second. Time in milliseconds.

shortening has certain limitations, since sarcomere length changes may not be uniform and the condition of the preparation is difficult to evaluate. Motility assays lack the mechanical constraints of position and separation on the actin–myosin interaction that exist within a myofilament lattice. It has been shown that lattice spacing changes occur as a result of force development and redevelopment in living fibers (17), which suggests a radial component of crossbridge force exists, whose magnitude varies with lattice spacing. The constraints imposed on the crossbridge cycle by lattice spacing and radial forces generated during activation are unknown, but are either absent or greatly modified in motility assays. The single intact fiber preparation avoids the problems of whole muscle, allowing precise measurement of sarcomere length, shortening, and tension development, while maintaining the highly structured arrangement of the contractile proteins which is lost in motility assays. It also permits the measurement of fiber stiffness with greater precision than is possible in whole muscle.

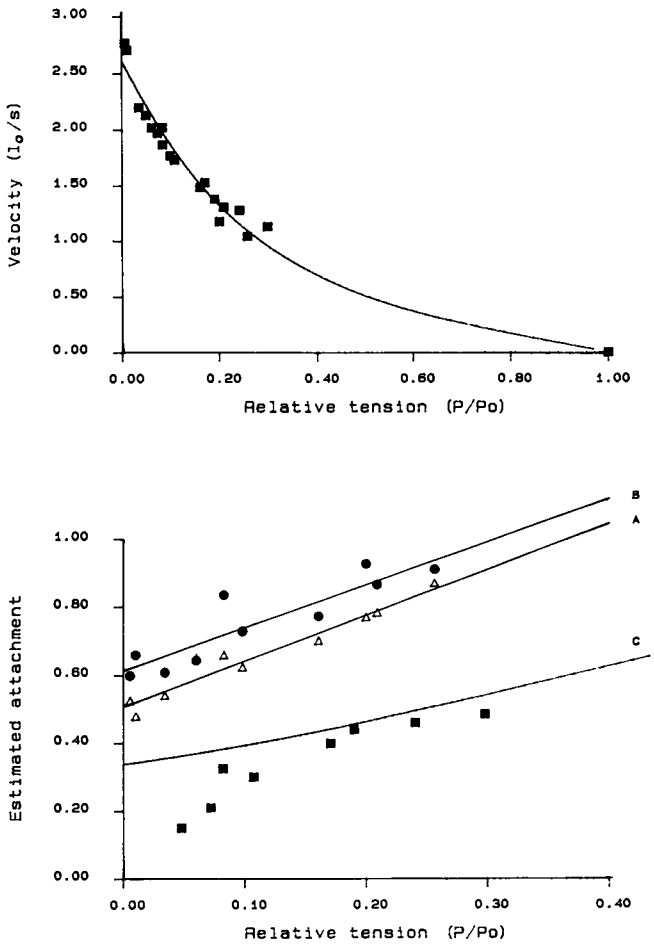

FIGURE 7 Top panel: force–velocity curve obtained from intact single fibers used in x-ray diffraction and stiffness measurements. Ordinate: Velocity in muscle lengths per second; abscissa: relative tension. The fitted line yields a V_{max} of 2.59 muscle lengths per second. Lower panel: normalized equatorial signals (I_{10}, △; I_{11}, ●) and stiffness (■) during isotonic shortening as a function of relative force (P/P_0). Data plotted from 8 fibers. The lines drawn through the intensity points are linear regression fits to the intensity in each case (*A*, 10; *B*, 11). The best fit gave values for the equatorial signals at zero relative force (i.e., V_{max}) of 60.65 ± 6.12% of the isometric signal for I_{10}, 50.76 ± 4.45% for I_{11} (95% confidence interval). The line close to the stiffness points (*C*) shows the expected fraction of attached crossbridges based on the best fit obtained of the force and velocity of shortening shown in the upper panel to the A. F. Huxley 1957 model (1) for the points plotted (f_1 + g_1 = 115 s^{-1}, g_2 = 337 s^{-1}, h = 15 nm) using a Marquardt–Levenberg fitting routine. At velocities close to V_{max}, stiffness falls away because of the increased contribution of tendon compliance to total stiffness. The stiffness at V_{max} is therefore obtained by extrapolation.

In the intact single fiber preparation under isometric conditions, the time courses of changes in both stiffness and equatorial signals during the rise of tetanic tension and relaxation are similar (6). Here we report a clear disagreement between these two putative measures of crossbridge attachment during shortening. As shortening velocity increases, stiffness falls off steadily to reach 30% of its isometric value at V_{max}, while the equatorial signals remain virtually unchanged at velocities less than 0.5 V_{max}, then fall to reach 51–61% of their isometric value at V_{max}. We will now consider some possible explanations for the disparity between the estimates of crossbridge attachment from these two techniques.

First, one should consider any intrinsic limitations in the estimation of attachment by x-ray diffraction. The dependence of equatorial intensities on the fraction of attached bridges has been shown only in the isometric case (5), and during shortening a population of bridges may exist whose structure gives rise to an equatorial pattern which causes us to overestimate the fraction of attached bridges. However, equatorial signals from both 10 and 11 reflections behave similarly, which is consistent with a change in the number of attached bridges (though not exclusively so). Since intensities are sensitive to lattice disorder and lattice spacing, these factors might cause us to underestimate the intensity change due to shortening, leading to the disparity between stiffness and intensity data. Our studies indicate that lattice spacing can affect intensities quite strongly, but the equatorial intensities which we have examined are all affected by about the same amount and in the same direction, increased during lattice expansion, reduced by lattice compression. It is known that the redevelopment of tension from the isotonic to the isometric state is associated with a lattice compression (17) at the plateau of the length tension relationship. However, since the intensity changes associated with shortening *per se* are in opposite directions for the 10 and 11 reflections, the effect of lattice expansion during shortening would be to cause the 10 signal to be overestimated, and the 11 signal to be underestimated. In Fig. 7, for example, correction for lattice spacing would tend to bring line *A* (for 10) and line *B* (for 11) closer together, but would not cause the corrected lines to approach the stiffness points and so cannot account for the disparity between stiffness and equatorial signals. As regards disorder, an indication of lattice disorder is a broadening of reflections proportional to the square of their distance from the origin of the pattern. An increase in this type of disorder can be detected in the transition from the relaxed to the isometric activated state in Fig. 4, where the 11 reflection broadens noticeably. Upon activation, the increased disorder may cause the 10 signal to be overestimated and 11 underestimated. We find that during shortening this disorder decreases only slightly, compared to the isometric tetanus plateau, even when isotonic force is close to zero, and so any effect of disorder on the absolute intensity change associated with the transition from isotonic to isometric contraction will be very small. Therefore, in comparison to the equatorial signal changes associated with activation, the change in the 11 signal associated with shortening would be overestimated, while that associated with 10 underestimated. In addition, since the effects of disorder are more pronounced on reflections fur-

ther from the origin of the diffraction pattern, the overestimation of the 11 signal change is probably larger than the underestimation of that of 10. The effect of this on Fig. 7 would be to cause the lines associated with the equatorial signals to diverge from one another, 10 points being displaced towards the stiffness points, 11 points being displaced by a somewhat greater amount away from the stiffness points. In view of the fact that both sets of equatorial signal points in Fig. 7 are rather close together, we think that disorder effects on the equatorial signals are not large, and would in any case not be able to explain the disparity in the estimate of crossbridge attachment obtained from the stiffness data.

It is also unlikely that the dependence of equatorial intensities on sarcomere length significantly influences our findings, since over the range of shortening in our experiments the relaxed state intensities are almost insensitive to sarcomere length, and in the activated state only a 2% change in intensity could be expected (Fig. 3). As can be seen in Figs. 5 and 6, a slight difference in isometric 10 intensity before and after shortening can be observed, which may result from the sarcomere length sensitivity of I_{10} in this range. The gradual increase in I_{10} and decrease in I_{11} with increasing sarcomere length in the activated state (Fig. 3 *b*) may be consistent with the reduction in the number of cycling bridges as the region of overlap becomes smaller. The very sharp decline in I_{11} in the relaxed state with increasing sarcomere length (Fig. 3 *a*), however, is much steeper than the change in filament overlap, and may be influenced by other factors. For example, changes in sarcomere length are accompanied by changes in lattice spacing, and therefore sampling of the form factor at different positions. This effect would also influence the sarcomere length dependence of I_{10} and I_{11}. In addition, increasing lattice disorder at longer sarcomere lengths could also contribute to a decline in I_{11}.

We will now consider possible physiological explanations for this disparity. Detached heads might remain in the vicinity of the actin filament during shortening, affecting the equatorial signals, either as a result of diffusional delays or activation-induced changes in crossbridge structure. It is known that in the relaxed state, the S1 head is freely mobile, and we calculate that the rotational and translational diffusion coefficients of S1 are fast enough to ensure a restoration of the relaxed state head distribution within a few microseconds of head detachment, so it is unlikely that diffusional delays following detachment cause an artificially high attached bridge estimate from the x-ray data. It is also known (19) that activation *per se* does not cause a change in equatorial intensities, and therefore cannot account for the disparity between stiffness and equatorial signals.

A further intriguing possible explanation of the disparity between stiffness and equatorial signals during shortening concerns the number of cycling heads. If it were assumed that in the isometric activated state, most crossbridges had both heads attached to the actin filament (either through cooperativity in binding, or because in the isometric state a large fraction of the crossbridge cycle time is spent in attached states), but during shortening a large population had only one head attached (the fraction of cycle time spent in attached states becoming much smaller than under isometric conditions), the free head might be displaced close to a neighboring actin filament, and so contribute to the diffraction pattern as if attached. If the stiffness of a two-headed attached bridge were the same as that of a bridge with only one head attached (i.e., stiffness proportional to the number of attached bridges), the proportion of attached bridges estimated from stiffness would be the same or greater than that estimated from the equatorial signals. If the two-headed bridge were twice as stiff as the bridge with only a single head attached (i.e., stiffness proportional to the number of heads attached), then the equatorial signals would suggest a greater degree of attachment than the stiffness measurements because of the propinquity of the detached head to an actin filament. The observations reported here would therefore be consistent with stiffness being dependent on the number of attached heads, since our equatorial signals do indicate higher levels of attachment than does stiffness. The use of stiffness as a measure of crossbridge attachment assumes that all forms of attached bridge have the same stiffness, so if isotonic bridges were less stiff than isometric, the degree of attachment would be underestimated by stiffness measurements.

Although inadequate for the description of isometric force transients, a simple two state crossbridge model can describe the isotonic condition quite well. The dependence of force and stiffness on shortening velocity is well fitted at steady state to the fraction of attached bridges predicted by the model of A. F. Huxley (1), as shown in Fig. 7. However, the transient solution of this model (20) describes neither the time course of the force transient nor the magnitude and time course of the approach of the equatorial signals to steady state values during shortening adequately, using the constants determined from the steady state fit. Application of the two-state model to motility assays leads to the predicted proportion of attached bridges rising during shortening at moderate to high velocities (13), since a reduction of crossbridge noise from a single actin filament during sliding is observed compared to the isometric case, which may result from a larger fraction of the ATPase cycle time being spent in force-generating states during shortening. This expectation is contrary to the behavior of both the stiffness and the equatorial signals in our findings, although these authors also report that shortening is associated with a large fall in stiffness. Clearly the two state model of A. F. Huxley (1) is inadequate to explain our findings, and when applied to motility assays leads to

estimates of crossbridge attachment during shortening which are at variance with both our stiffness and our x-ray signals.

The analysis of the behavior of fluorescently labeled actin filaments in free motion on a field of myosin heads indicates at least 75% of the ATPase cycle time is spent in force-producing states (12). This value is comparable to that predicted under isometric conditions (21), and would require a large working stroke for the attached crossbridge. A means of avoiding such a long working stroke time might be found if force were exerted by "weakly bound" crossbridge states (12), which could achieve several attachment/detachment cycles during one ATPase cycle time. We consider this unlikely to occur in living cells, since it is known that these "weakly bound' states" are present only in very small amounts at physiological ionic strength in frog muscle, and that their equilibrium kinetics are very fast (22). It can be shown that the frequency response of the stiffness of weakly bound bridges as measured by sinusoidal length oscillations can be described by the equation (22, 23):

$$M(f) = 2\pi f/(k_b^2 + 4\pi^2 f^2)^{1/2}$$

where k_b is the detachment rate constant, f the frequency of sinusoidal length oscillations used to measure stiffness. If k_b is 10^4 s^{-1} (22), at 4 kHz we would expect to detect 93% of weak bridge stiffness, hence stiffness and equatorial signals should be almost equal. Nevertheless, a multiple state model containing a strongly bound attached state with sufficiently fast equilibrium kinetics to be largely invisible to stiffness measurements at 4 kHz would account for the disparity between x-ray and stiffness data.

Whatever the cause of the difference between stiffness and equatorial signals, the absence of a pronounced effect of shortening on intensity data reported previously (7) from whole sartorius muscles of *Rana temporaria* is largely consistent with our findings. The load during shortening in their experiments was never smaller than 0.14 P_0, which, from Fig. 7, would cause a change in equatorial signals of at most 25%, and less than 10% at 0.25 P_0 or above. Furthermore, they were unable to exclude the period required to reach steady state intensity from their data collection during shortening, which would cause an underestimation of the intensity change at any given shortening velocity. The dependence of equatorial signals on force during shortening reported here is smaller than that previously reported (8) in whole sartorius muscles of *Rana pipiens,* where a fall in equatorial signals to 50% of their isometric level during shortening at 0.1 P_0 was found, whereas we obtain a fall to only 51–61% of isometric signals even when shortening at close to V_{max}. Although quantitatively different from our results, these previous studies support our finding that changes in equatorial intensities during shortening are smaller than the accompanying changes in fiber stiffness, and that therefore in the isotonic state one of these two techniques is an unsuitable measure of crossbridge attachment.

The authors are indebted to the members of the European Molecular Biology Laboratory Outstation in Hamburg for their expert assistance in this project, and to Mr Paolo Garzella for helpful suggestions and discussions.

Supported by the Medical Research Council, European Molecular Biology Laboratory, Consiglio Nazionale di Recherche, and the National Institutes of Health.

Received for publication 17 August 1992 and in final form 21 December 1992.

REFERENCES

1. Huxley, A. F. 1957. Muscle structure and theories of contraction. *Prog. Biophys. Biophys. Chem.* 7:255–318.
2. Huxley, H. E. 1969. The mechanism of muscle contraction. *Science (Wash. DC).* 164:1356–1366.
3. Huxley, A. F., and R. M. Simmons. 1971. Proposed mechanism of force generation in striated muscle. *Nature (Lond.).* 213:533–538.
4. Haselgrove, J. C., and H. E. Huxley. 1973. X-ray evidence for radial cross-bridge movement and for the sliding filament model in actively contracting skeletal muscle. *J. Mol. Biol.* 77:549–568.
5. Yu, L. C., J. E. Hartt, and R. J. Podolsky. 1979. Equatorial X-ray intensities and isometric force levels in frog sartorius muscle. *J. Mol. Biol.* 132:53–67.
6. Cecchi, G., P. J. Griffiths, M. A. Bagni, C. C. Ashley, and Y. Maéda. 1991. Time-resolved changes in equatorial x-ray diffraction and stiffness during rise of tetanic tension in intact length-clamped single muscle fibers. *Biophys. J.* 59:1273–1283.
7. Podolsky, R. J., R. St. Onge, L. C. Yu, and R. W. Lymn. 1976. X-ray diffraction of actively shortening muscle. *Proc. Nat. Acad. Sci. USA.* 73:813–817.
8. Huxley, H. E., M. Kress, A. F. Faruqi, and R. M. Simmons. 1986. X-ray diffraction studies on muscle during rapid shortening and their implications concerning cross-bridge behaviour. *Adv. Exp. Med. Biol.* 226:347–352.
9. Julian, F. J., and M. R. Sollins. 1975. Variation of muscle stiffness with force at increasing speeds of shortening. *J. Gen. Physiol.* 66:287–302.
10. Julian, F. J., and D. L. Morgan. 1981. Variation of muscle stiffness with tension during tension transients and constant velocity shortening in the frog. *J. Physiol. (Lond.).* 319:193–203.
11. Ford, L. E., A. F. Huxley, and R. M. Simmons. 1985. Tension transients during steady shortening of frog muscle fibres. *J. Physiol. (Lond.).* 361:131–151.
12. Harada, Y., K. Sakurada, T. Aoki, D. D. Thomas, and T. Yanagida. 1990. Mechanochemical coupling in actomyosin energy transduction studied by *in vitro* movement assay. *J. Mol. Biol.* 216:49–68.
13. Ishijima, A., T. Doi, K. Sakurada, and T. Yanagida, T. 1991. Sub-picoNewton force fluctuations of actomyosin *in vitro*. *Nature (Lond.).* 352:301–306.
14. Cecchi, G., P. J. Griffiths, and S. R. Taylor. 1986. Stiffness and

force in activated frog skeletal muscle fibres. *Biophys. J.* 49:437–451.

15. Hendrix, J., H. Fuerst, B. Hartfiel, and D. Dainton. 1982. A wire per wire detector system for high counting rate X-ray experiments. *Nucl. Inst. Methods.* 201:139–144.
16. Yu, L. C., A. C. Steven, G. R. S. Naylor, R. C. Gamble, and R. J. Podolsky. 1985. Distribution of mass in relaxed frog skeletal muscle and its redistribution upon activation. *Biophys. J.* 47:311–321.
17. Cecchi, G., M. A. Bagni, P. J. Griffiths, C. C. Ashley, and Y. Maéda. 1990. Detection of radial crossbridge force by lattice spacing changes in intact single muscle fibers. *Science (Wash. DC).* 250:1409–1411.
18. Bagni, M. A., G. Cecchi, F. Colomo, and C. Tesi. 1988. The mechanical characteristics of the contractile machinery at different levels of activation in intact single muscle fibres of the frog. *Adv. Exp. Med. and Biol.* 226:473–487.
19. Huxley, H. E. 1979. Time-resolved x-ray diffraction studies on muscle. In *Cross-bridge Mechanism in Muscle Contraction.* H. Sugi and G. H. Pollack, editors. University Park Press, Baltimore. 391–405.
20. Zahalek, G. I. 1981. A distribution-moment approximation for kinetic theories of muscle contraction. *Math. Biosci.* 55:89–114.
21. Goldman, Y. E., and R. M. Simmons. 1977. Active and rigor stiffness. *J. Physiol. (Lond.).* 269:55*P.*
22. Schoenberg, M. 1988. Characterization of the myosin adenosine triphosphate (M.ATP) crossbridge in rabbit and frog skeletal muscle fibers. *Biophys. J.* 54:135–148.
23. Schoenberg, M. 1991. Mechanical detection of weakly-binding M.ATP crossbridges. *Biophys. J.* 59:51*a.*